

## EFFECT OF POSITRON RANGE ON SPATIAL RESOLUTION

Michael E. Phelps, Edward J. Hoffman, Sung-Cheng Huang, and Michel M. Ter-Pogossian

Washington University School of Medicine, St. Louis, Missouri

*The effect of  $\beta^+$  range on spatial resolution of imaging systems employing the detection of 511-keV annihilation radiation was determined by measuring the variation in the line-spread functions (LSFs) of positron-emitting radionuclides of  $^{64}\text{Cu}$ ,  $^{11}\text{C}$ , and  $^{15}\text{O}$  as compared with the 514-keV gamma-ray emitter  $^{85}\text{Sr}$ . These radionuclides have maximum  $\beta^+$  energies of 0.656, 0.960, and 1.72 MeV, respectively. The LSFs were measured in a tissue-equivalent phantom with high-resolution ( $\sim 2.4$  mm FWHM) and low-resolution ( $\sim 8.8$  mm FWHM) straight-bore collimators coupled to a NaI(Tl) detector. Theoretical LSFs for the  $\beta^+$  ranges were also calculated and convolved with the  $^{85}\text{Sr}$  LSF to yield the predicted LSFs for  $^{11}\text{C}$  and  $^{15}\text{O}$ . The high-resolution study showed a 0% and 2.3% increase in the full-width half-maximum (FWHM) and full-width tenth-maximum (FW0.1M) for the low-energy  $\beta^+$  of  $^{64}\text{Cu}$  and a 37% (FWHM) and 52% (FW0.1M) increase for the high energy  $\beta^+$  of  $^{15}\text{O}$  as compared with  $^{85}\text{Sr}$ . However, when the system resolution was decreased to 8.8 mm FWHM, the  $^{64}\text{Cu}$  showed no change at FWHM or FW0.1M and the  $^{15}\text{O}$  showed a 2.3% (FWHM) and 7.8% (FW0.1M) relative to  $^{85}\text{Sr}$ . The predicted LSFs were in good agreement with the experimental. These data indicate that the effect of  $\beta^+$  range on spatial resolution is minimal unless the  $\beta^+$  energy is  $\geq 1.5$  MeV and the system resolution is on the order of a few millimeters.*

plication of these systems to transaxial reconstruction tomography (4–9). Since the radiation utilized in the imaging of positron-emitting radionuclides is a result of annihilation of a positron with an electron, the origin of the radiation is not the position of the radionuclide but some distance from it due to the finite range of the  $\beta^+$ . The effect of the  $\beta^+$  range is to limit the spatial resolution of the imaging device. Whether or not this limit in resolution is of consequence in nuclear medicine imaging is the subject of this work.

To evaluate the magnitude of this effect, we have measured the line-spread functions (LSFs) of the positron-emitting radionuclides of  $^{64}\text{Cu}$ ,  $^{11}\text{C}$ , and  $^{15}\text{O}$  with maximum  $\beta^+$  energies of 0.656, 0.960, and 1.72 MeV, respectively. The LSFs were measured with two straight-bore collimators with full-width half-maximum (FWHM) resolution of approximately 2.4 and 8.8 mm. These results are compared with the LSFs of  $^{85}\text{Sr}$  which emits a 514-keV gamma ray.

A theoretical model is also developed to calculate that part of the LSF due only to the range of the positrons. The theoretical LSFs for  $^{11}\text{C}$  and  $^{15}\text{O}$   $\beta^+$  ranges were convolved with the  $^{85}\text{Sr}$  LSF for comparison with the measured LSFs for these radionuclides.

### METHODS

**Theoretical LSF for  $\beta^+$  range.** The positron-emitting radionuclides of  $^{64}\text{Cu}$ ,  $^{11}\text{C}$ , and  $^{15}\text{O}$  were chosen since they emit positrons with a range of energies including most of the positron emitters considered to be candidates for radiopharmaceuticals. They have maximum positron energies ( $E_{\text{MAX}}$ ) from

Interest in positron-emitting radiopharmaceuticals for nuclear medicine imaging has increased with the development of devices suited for the detection of 511-keV annihilation radiation (1–3) and the ap-

Received Nov. 20, 1974; revision accepted Jan. 22, 1975.

For reprints contact: M. E. Phelps, Div. of Radiation Sciences, The Edward Mallinckrodt Institute of Radiology, St. Louis, Mo. 63110.

**TABLE 1. MAXIMUM AND AVERAGE POSITRON ENERGIES AND RANGES**

Isotope	Maximum $\beta^+$ energy $E_{Max}$ (MeV)	Average $\beta^+$ energy (MeV)	Maximum range* $R_{Max}$ (mm)	Range of average $\beta^+$ energy (mm)
$^{64}\text{Cu}$	0.656	0.262	2.4	0.64
$^{11}\text{C}$	0.960	0.384	3.9	1.1
$^{15}\text{O}$	1.720	0.688	7.9	2.5

\* Linear range in water.

0.656 to 1.72 MeV (10) and corresponding maximum linear ranges ( $R_{Max}$ ) in water of 2.4–7.9 mm (11) as shown in Table 1. However, these maximum  $\beta^+$  energies and ranges are misleading in this context for several reasons: (A) positrons are emitted with a spectrum of energies from zero to  $E_{Max}$  with the average energies occurring at 0.4  $E_{Max}$ ; (B) positrons are emitted isotropically which effectively compresses their range when viewed two-dimensionally; and (C) the range of the positron is through a tortuous path due to collisions with atomic electrons and the nuclei of the surrounding media and this reduces the net linear range of the positron since the range  $R$  is for a straight-line path. Thus, the average range of the positrons from a given radionuclide is considerably smaller than one might expect when only  $E_{Max}$  and  $R_{Max}$  are taken into consideration.

The above effects were taken into account in calculating the LSFs for the positron range by assuming that the number of positrons decreases with distance by the exponential relationship:

$$I/I_0 = e^{-\mu x}, \quad (1)$$

where  $x$  is the linear distance from the point of emission and  $\mu$  is the linear-attenuation coefficient. Equation 1 is given by Evans (11) as a good approximation for the continuous distribution of  $\beta^-$  particles. However, the average energy of positrons is higher ( $\sim 0.4 E_{Max}$ ) than that of  $\beta^-$  ( $\sim 0.3 E_{Max}$ ). Thus the value of  $\mu$  for the positrons was chosen by using the value of (11) of  $\mu$  for a  $\beta^- E_{Max}$  adjusted by the ratio of the average energy of  $\beta^+$  to  $\beta^-$  ( $E_{Max}$  0.4/0.3). Equation 1 collectively takes into account the continuous distribution of  $\beta^+$  energies and the non-linear path. Using Eq. 1 and the isotropic emission of positrons, the LSFs for the positron range of  $^{11}\text{C}$  and  $^{15}\text{O}$  were calculated. The LSF for the  $\beta^+$  range of  $^{11}\text{C}$  had a FWHM and FWO.1M of 0.33 mm and 1.3 mm, respectively, as shown in Fig. 1. The LSF shown in Fig. 1 illustrates the small overall effect of positron range on broadening the response. The

LSFs for the  $\beta^+$  ranges of  $^{11}\text{C}$  and  $^{15}\text{O}$  were convolved with the experimental  $^{85}\text{Sr}$  LSF to yield a theoretical total LSF for these positron-emitting radionuclides. These theoretical LSFs were compared with the experimental measurements.

**Experimental LSF of  $\beta^+$  range.** The LSFs for  $^{85}\text{Sr}$ ,  $^{64}\text{Cu}$ ,  $^{11}\text{C}$ , and  $^{15}\text{O}$  were measured with a high- and a low-resolution system. The high-resolution system ( $\sim 2.4$  mm FWHM) was used to measure accurately the effect of the  $\beta^+$  range and the low-resolution system ( $\sim 8.8$  mm FWHM) to measure the effect of  $\beta^+$  range on a resolution which is comparable to the best overall resolution presently available in nuclear medicine.

The high-resolution system consisted of a shielded 1 cm  $\times$  5 cm NaI(Tl) detector placed behind a 5-cm-thick lead brick with a straight-bore hole which was 2 mm  $\times$  5 cm. The line source consisted of a 4-cm plastic cube (density = 1.05 gm/cc) with a hole 1.5 mm  $\times$  2 cm containing the appropriate radionuclide. The cube was placed against the face of the collimator and the distance between the line source and collimator was 1 cm. The 1-cm distance between the line source and collimator was chosen to provide a thickness of absorbing medium greater than the maximum range of the  $\beta^+$  particles used in this work (Table 1). The low-resolution system was identical to the high-resolution system except that the plastic cube was 5 cm on a side, the line source was 1.5 mm  $\times$  4 cm, and the straight-bore collimator was 8 mm  $\times$  7.5 cm.

The line source was automatically scanned by the collimator with a computer-controlled scanning table at steps of 0.25 mm. The output of the NaI(Tl)

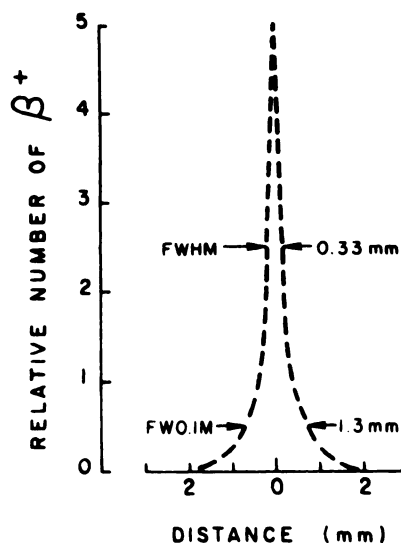


**FIG. 1.** Theoretical LSF for range of  $\beta^+$  from  $^{11}\text{C}$  in tissue-equivalent media (density = 1.05 gm/cc).

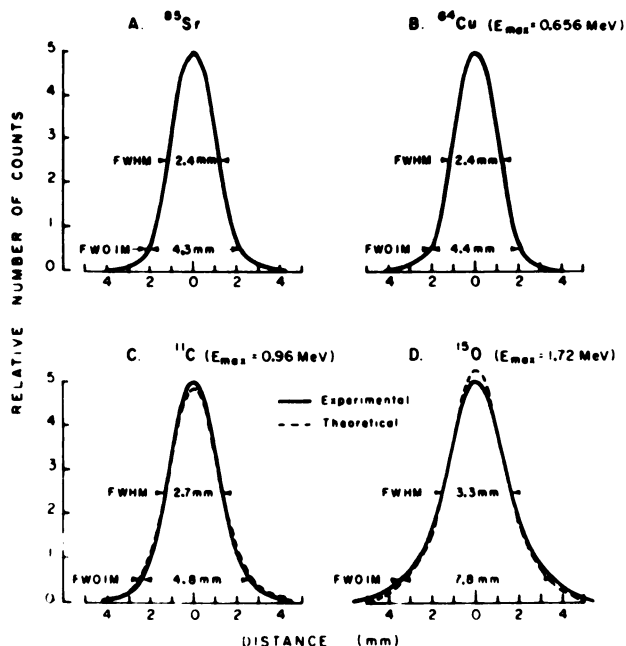


**FIG. 2.** Solid lines: experimental LSFs of  $^{85}\text{Sr}$ ,  $^{64}\text{Cu}$ ,  $^{11}\text{C}$ , and  $^{15}\text{O}$  with high-resolution collimator. Dashed lines: predicted LSFs for  $^{11}\text{C}$  and  $^{15}\text{O}$  from convolving theoretical  $\beta^+$  range LSFs (e.g., Fig. 1) with  $^{85}\text{Sr}$  experimental LSF (tissue-equivalent media).

detector was processed by a preamplifier, amplifier, and single-channel analyzer (window of 470–551 keV). The output of the single-channel analyzer was collected by an on-line computer that also corrected for background and radioactive decay.

#### RESULTS AND DISCUSSION

The LSFs for  $^{85}\text{Sr}$ ,  $^{64}\text{Cu}$ ,  $^{11}\text{C}$ , and  $^{15}\text{O}$  taken with the high-resolution system are shown in Fig. 2 as solid lines. Using the 514-keV gamma ray of  $^{85}\text{Sr}$  as representing the geometric and detector response, one can see the increase in FWHM and FW0.1M as the  $E_{\text{Max}}$   $\beta^+$  energy increases from 0.656 to 1.72 MeV of  $^{64}\text{Cu}$  and  $^{15}\text{O}$ , respectively. Increases of 37% (FWHM) and 52% (FW0.1M) were observed in the worst case of the high-energy positrons of  $^{15}\text{O}$  when compared with the  $^{85}\text{Sr}$  with the high-resolution collimator. The lower energy  $\beta^+$  emitter  $^{64}\text{Cu}$  showed increases of  $\sim 0\%$  and 2.3% at the FWHM and FW0.1M compared with  $^{85}\text{Sr}$ .

The predicted LSFs for the  $^{11}\text{C}$  and  $^{15}\text{O}$  obtained by convolving the calculated  $\beta^+$  range LSF (METHODS section) with the  $^{85}\text{Sr}$  LSF are shown as dashed lines in Fig. 2. These predicted curves agree well with the experimental ones.

When the spatial resolution of the system is decreased to 8.8 mm, the loss in spatial resolution from the  $\beta^+$  range is less marked than in the previously mentioned case. The FWHM and FW0.1M for the worst case of  $^{15}\text{O}$  increased by 2.3% and 7.8%, re-

spectively, and no change was observed for  $^{64}\text{Cu}$  relative to  $^{85}\text{Sr}$  as shown in Fig. 3.

#### CONCLUSION

The effect of positron range in spatial resolution is significant if high-energy, positron-emitting radionuclides ( $E_{\text{Max}} \geq 1.5$  MeV) are employed with imaging devices with overall resolution of a few millimeters (Fig. 2). However, this effect is rapidly diminished as the spatial-resolution capabilities of the imaging device are decreased. Even with an overall resolution of  $\sim 8.8$  mm, which is better than any imaging devices presently employed in nuclear medicine, the effect of  $\beta^+$  range is minor (Fig. 3). Oxygen-15 with a 1.72-MeV  $E_{\text{Max}}$  increased the FWHM and FW0.1M resolution by 2.3 and 7.8%, respectively, and no effect was observed for  $^{64}\text{Cu}$  ( $E_{\text{Max}} = 0.656$  MeV) as compared with the gamma-ray emitter  $^{85}\text{Sr}$ . The results of Cho, et al (13) on the effect of positron range on spatial resolution are in good agreement with the work presented here.

Graham, et al (12) using a Picker Dynacamera with a pinhole collimator found a negligible effect on spatial resolution using  $^{18}\text{F}$ ,  $^{11}\text{C}$ , and  $^{13}\text{N}$  compared with  $^{85}\text{Sr}$ .

It should be pointed out that even if high-resolution (few millimeters) imaging devices are developed, the image will only represent this resolution if a corresponding statistical level of data is attained. This will be a difficult task in the photon-limited field of nuclear medicine imaging unless an extremely high efficiency is associated with the high resolution since

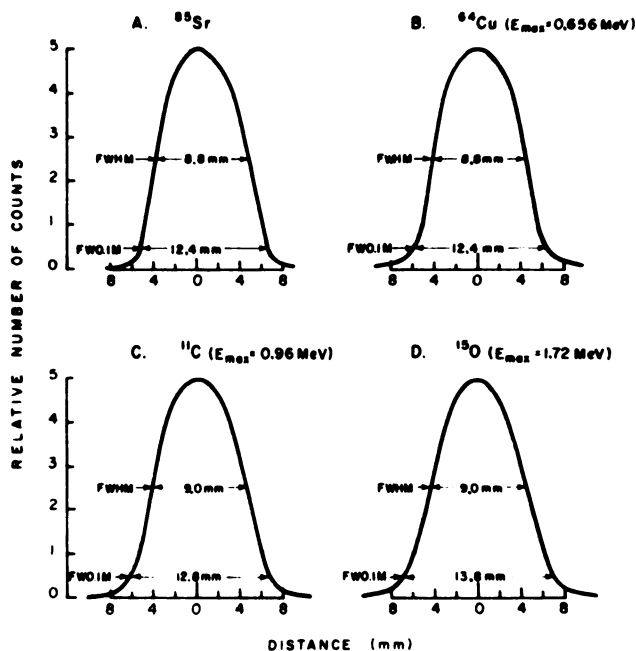


**FIG. 3.** Experimental LSFs for  $^{85}\text{Sr}$ ,  $^{64}\text{Cu}$ ,  $^{11}\text{C}$ , and  $^{15}\text{O}$  with low-resolution collimator (tissue-equivalent media).

the photon requirement generally varies by the reciprocal of resolution to the fourth power.\*

The effect of  $\beta^+$  range in spatial resolution as presented in this work explicitly applies to most soft tissues and body fluids that have densities around 1 gm/cc. The exception to this are bone which will further decrease the effect of  $\beta^+$  range due to its higher density ( $\sim 1.7$  gm/cc) and lung which will increase the effect of  $\beta^+$  range due to its lower density ( $\sim 0.36$  gm/cc). The LSF for the worst case of  $^{15}\text{O}$  in lung tissues would add about 0.2 mm to the FWHM and about 1.6 mm to the FW0.1M of the low-resolution LSF shown in Fig. 3.

#### ACKNOWLEDGMENTS

This work was supported by NIH Grant No. 5 P01 HL13851, by the National Institutes of Health, by NIH Grant No. 1 R01 HL 15423, by NIH Fellowship No. (1-F)-3-GM55196, and NIH Research Grant RR-00396 from the Division of Research Resources.

#### REFERENCES

1. BROWNELL GL, BURNHAM CA: MGH positron camera. In *Tomographic Imaging in Nuclear Medicine*, Freedman GS, ed, New York, Society of Nuclear Medicine, 1974, pp 154-164

\* The number of resolution elements in the image increases by the square of the resolution and the detection efficiency also varies by the square of the resolution.

2. BURNHAM CA, ARONOW S, BROWNELL GL: A hybrid positron scanner. *Phys Med Biol* 15: 517-528, 1970
3. MONAHAN WG, BEATTIE JW, LAUGHLIN JS: Positron mode of the total organ kinetic imaging monitors: System design and applications. *Phys Med Biol* 17: 503-513, 1972
4. CHESLER DA: Positron tomography and three dimensional reconstruction techniques. In *Tomographic Imaging in Nuclear Medicine*, Freedman GS, ed, New York, Society of Nuclear Medicine, 1974, pp 176-183
5. CORMACK AM: Reconstruction of densities from their projections with applications in radiological physics. *Phys Med Biol* 18: 195-207, 1973
6. PHELPS ME, HOFFMAN EJ, MULLANI N, et al: Application of annihilation coincidence detection to transaxial reconstruction tomography. *J Nucl Med* 16: 210-224, 1975
7. TER-POGOSSIAN MM, PHELPS ME, HOFFMAN EJ, et al: A positron emission tomograph for nuclear medicine imaging (PETT). *Radiology* 114: 89-98, 1975
8. ROBERTSON JS, MARR RB, ROSENBLUM M, et al: 32-crystal positron transverse section detection. In *Tomographic Imaging in Nuclear Medicine*, Freedman GS, ed, New York, Society of Nuclear Medicine, 1974, pp 142-153
9. CHO ZH: 3-Dimensional image reconstruction algorithm for nuclear medicine imaging processing using transmission and emission. *Instrumentation* 2: 1262-1263, 1974
10. LEDERER MC, HOLLANDER JC, PERLMAN I: *Table of Isotopes*, 6th ed, New York, Wiley, 1967
11. EVANS RD: *The Atomic Nucleus*. New York, McGraw-Hill, 1955, pp 621-628
12. GRAHAM LS, MACDONALD NS, ROBINSON GD, et al: Personal communication, 1974
13. CHO ZH, CHAN JK, ERIKSON L, et al: Positron ranges obtained from biomedically important positron-emitting radionuclides: Unpublished data